Submitted to Nature Chemistry for consideration as a Research Article.

Constructing ion-channels from water-soluble α–helical barrels

Alistair J. Scott[1,†], Ai Niitsu[1,2,†], Huong T. Kratochvil[3,§], Eric J. M. Lang[1,§], Jason T. Sengel[4,§], William M. Dawson[1], K. R. Mahendran[5,6], Marco Mravic[3], Andrew R. Thomson[1,7], R. Leo Brady[8,9], Lijun Liu[10,11], Adrian J. Mulholland[1,9], Hagan Bayley[5], William F. DeGrado[3], Mark I. Wallace[4], and Derek N. Woolfson[1,8,9,*]

[†]These authors contributed equally to this work.
[§]These authors contributed equally to this work.
*Corresponding author. Email: d.n.woolfson@bristol.ac.uk

[1]School of Chemistry, University of Bristol, Cantock's Close, Bristol, BS8 1TS, UK.

[2]Present address: Theoretical Molecular Science Laboratory, RIKEN Cluster for Pioneering Research, RIKEN, 2-1 Hirosawa, Wako, Saitama 351-0198, Japan.

[3]Department of Pharmaceutical Chemistry, University of California San Francisco, San Francisco, CA 94158, USA

[4]Department of Chemistry, King's College London, Britannia House, 7 Trinity Street, London, SE1 1DB, UK.

[5]Department of Chemistry, University of Oxford, Chemistry Research Laboratory, Mansfield Road, Oxford, OX1 3TA, UK.

[6]Present address: Membrane Biology Laboratory, Interdisciplinary Research Program, Rajiv Gandhi Centre for Biotechnology, Thiruvananthapuram, 695014, India.

[7]Present address: School of Chemistry, Joseph Black Building, University Avenue, Glasgow G12 8QQ, UK.

[8]School of Biochemistry, University of Bristol, Medical Sciences Building, University Walk, Bristol, BS8 1TD, UK.

[9]Bristol BioDesign Institute, University of Bristol, Life Sciences Building, Tyndall Avenue, Bristol BS8 1TQ, UK.

[10] School of Chemical Biology and Biotechnology, Peking University Shenzhen Graduate School, Shenzhen 518055, Peoples Republic of China.

[11]DLX Scientific, Lawrence, KS 66049, USA

The design of peptides that assemble in membranes to form functional ion channels is challenging. Specifically, hydrophobic interactions must be designed between the peptides and at the peptide-lipid interfaces simultaneously. Here, we take a multi-step approach towards this problem. First, we use rational *de novo* design to generate water-soluble α-helical barrels with polar interiors, which are confirmed to high resolution by X-ray crystallography. These have water-filled lumens like those of transmembrane channels. Then, we modify the sequences to facilitate their insertion into lipid bilayers. Single-channel electrical recordings and fluorescent imaging of the peptides in membranes show monodisperse, cation-selective channels of unitary conductance. Surprisingly, however, an X-ray structure solved from lipidic cubic phase for one peptide reveals an alternate state with tightly packed helices and a constricted channel. To reconcile these observations, we perform computational analyses to compare the properties of possible different states of the peptide.

The *de novo* design of water-soluble proteins has progressed rapidly[1,2]. In comparison, membrane protein design is less developed. Indeed, relatively few *de novo* membrane proteins have been defined in structural detail: helical bundles have been specified by computationally designed hydrogen-bond networks[3] or side-chain packing[4], and a Zn^{2+}/ H^{+} antiporter has been achieved[5]. Moreover, many natural membrane proteins respond to chemical and physical cues; *e.g.*, G-protein coupled receptors, ligand- and voltage-gated ion channels, and water-soluble toxins that form membrane-spanning pores. The *de novo* design of such multi-state systems is particularly challenging[6,7].

The self-assembly of *de novo* α-helical peptides presents an attractive route to address the challenge of designing transmembrane proteins. This is because established structural principles for α-helical folding and assembly provide starting points for design[2,8]. Nonetheless, there are relatively few successful *de novo* designs of functional transmembrane peptides such as ion channels[9,10]. Advancing the design field to deliver such targets requires solutions to three interlinked design challenges: first, helix-helix interactions must be specified to maintain discrete oligomers; second, this has to be done in competition with interactions needed to interface the structures with lipids; third, the assemblies must have accessible, water-filled lumens lined with polar residues, which may compromise helix-helix packing and structural stability. Moreover, a particular challenge is that this all has to be encoded within approximately 30-residue peptides, the length required for an α helix to span a lipid bilayer[11,12].

Here, we combine rational and computational design to produce peptides that self-assemble into water-soluble α-helical barrels. These have polar lumens wetted by dynamic networks of water molecules. With insights from these structures, we introduce outwardly projecting hydrophobic residues to generate membrane-spanning peptides. These form well-defined ion channels that conduct approximately 10^8 ions per second. These are the first examples of modifying water-soluble, self-assembling *de novo* peptides to facilitate membrane insertion; though non-functional *de novo* proteins have been altered similarly to facilitate membrane insertion[3]. Moreover, in membranes, the peptides form channels with lifetimes unprecedented for designed systems, allowing their dynamics to be imaged directly. We present a crystal structure for one peptide assembly from the lipidic cubic phase. This reveals an unanticipated alternate state with tightly packed helices. This is almost certainly a non-conducting state. To reconcile these data, we use computational analyses to develop a model for the peptide's structure and activity. We posit that the multiple states observed can be understood in terms of the relative energetics of helix-packing interactions in water-soluble and membrane proteins, and possibly the influence of vectorial insertion of peptides into membranes. This study highlights the challenges of designing discrete membrane-spanning ion channels from self-assembling peptides, which we discuss and place in a wider context.

Results and discussion

Water-soluble α-helical barrels with solvated channels can be designed

To start the design process, we targeted α-helical-barrel (αHB) coiled-coil peptides. These have 'Type-2' heptad sequence repeats of hydrophobic (***h***) and polar (***p***) residues, ***hpphhph*** (labelled ***abcdefg***), which assemble into bundles of five or more α helices[13,14]. Previously, we have developed design principles and methods for water-soluble and membrane-spanning αHBs[4,15]. These exploit tight interhelical packing of mostly hydrophobic residues to specify the association states and internal radii of the assemblies. This packing stabilizes the structures, but it precludes their use as ion-channels. Therefore, we sought to place polar residues capable of favourable interactions with water into the lumens of αHBs.

We took a canonical water-soluble αHB (CC-Hept[15], systematically named CC-Type2-$(L_aI_d)_4$), with the following features (Fig. 1a and Table 1): Hydrophobic Leu at ***a*** and Ile at ***d*** point into the lumen but also stabilize interactions between neighbouring helices; small hydrophobic Ala residues at ***e*** and ***g*** supplement the helical interfaces to specify high-order bundles; and interactions between charged Lys and Glu side chains at ***b*** and ***c*** contribute further to the interfaces and provide water solubility. We explored placing neutral polar side chains at the lumenal ***a*** and ***d*** sites in this background (Fig. 1, Table 1, and Supplementary Table 1).

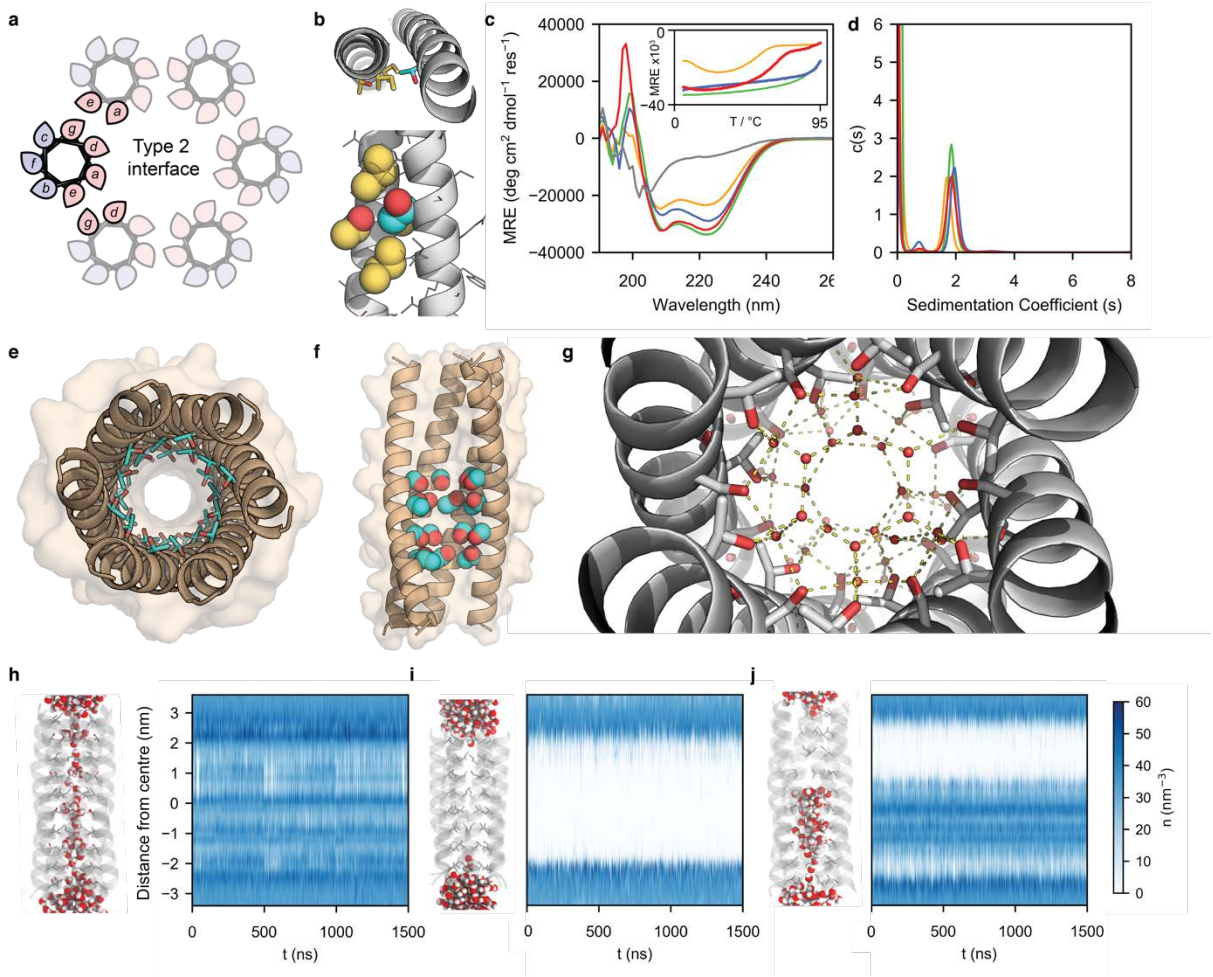

Fig. 1: Computational design and characterisation of water-soluble αHBs with solvated lumens. a, Helical wheels for parallel Type-2 coiled-coil interfaces with hydrophobic and polar residues shaded pink and blue, respectively. **b**, CCBuilder2 model of CC-Type2-$(L_aI_d)_4$ with Thr residues at one ***a*** site. Backbone parameters were from CC-Type2-$(L_aI_d)_4$ (PDB code: 4PNA) with side chains repacked using SCWRL4[16]. Knobs and holes residues are coloured cyan and gold, respectively. **c**, CD spectra at 20 ˚C and thermal denaturation profiles (inset) and (**d**) sedimentation velocity AUC c(s) distributions for CC-Type2-$(T_aI_d)_5$ (orange), CC-Type2-$(L_aT_d)_5$ (green), CC-Type2-$(S_aI_d)_5$ (gray), CC-Type2-$(L_aS_d)_5$ (blue), CC-Type2-$(T_aS_d)_2$ (red). **e**, 1.9 Å X-ray crystal structure of CC-Type2-$(T_aI_d)_5$ with internal Thr side chains shown as sticks. **f**, 1.9 Å X-ray crystal structure of CC-Type2-$(T_aS_d)_2$ with Thr and Ser side chains space-filled, and front two helices removed. **g**, Hydrogen-bonding water network in the lumen of the

crystal structure of CC-Type2-$(T_aS_d)_2$; hydrogen bonds (yellow dashes) are for O-O distances < 3 Å. **h – j**, Molecular dynamics of water ingress into the cavities of CC-Type2-$(T_aI_d)_5$ (**h**), CC-Type2-$(L_aI_dS_g)_4$ (**i**) and CC-Type2-$(T_aS_d)_2$ (**j**). Left-hand sides: representative snapshots after equilibration, with water molecules space filled and the *N* termini of the helices at the top. Plots: water number density (n) profiles for the channels generated using CHAP[17].

Because β-branched side chains at ***a*** and ***d*** help maintain open barrels[18], first we explored β-branched and polar Thr residues at these sites. Computational design[19] indicated that Thr at ***a*** was compatible with the knobs-into-holes (KIH) packing of coiled coils[20] and that the β-hydroxyl group projected into the lumen (Fig. 1b), whereas Thr at ***d*** could not assume this arrangement. To test this, we synthesized two peptides with Thr at five consecutive ***a*** or ***d*** positions, CC-Type2-$(T_aI_d)_5$ and CC-Type2-$(L_aT_d)_5$ (Table 1, and Supplementary Fig. 1). We examined their folding and assembly by far-UV circular dichroism (CD) spectroscopy and analytical ultracentrifugation (AUC); and we probed the binding of the environment-sensitive dye 1,6-diphenyl-1,3,5-hexatriene (DPH), which binds to open barrels but not to collapsed bundles[18]. Both peptides formed helical oligomers (Fig. 1c,d, Table 1, and Supplementary Fig. 2,3), but only CC-Type2-$(T_aI_d)_5$ bound DPH (Supplementary Fig. 4).

Name	Sequence	Helical	Binds DPH	Oligomer	PDB Code
Water-soluble	*cdefgab cdefgab cdefgab cdefgab cdefgab*				
CC-Type2-$(L_aI_d)_4$	G EIAKALK EIAKALK EIAWALK EIAKALK G	Yes	Yes	7	4PNA
CC-Type2-$(L_aI_dS_g)_4$	G EIAKSLK EIAKSLK EIAWSLK EIAKSLK G	Yes	Yes	6	4PN9
CC-Type2-$(T_aI_d)_2$	G EIAQALK EIAKA**T**K EIAWA**T**K EIAQALK G	Yes	N.D.	6	6YB2
CC-Type2-$(T_aI_d)_5$	G EIAQA**T**K EIAQA**T**K EIAKA**T**K EIAWA**T**K EIAQA**T**K G	Yes	Yes	6	6YAZ
CC-Type2-$(L_aT_d)_5$	G E**T**AQALK E**T**AQALK E**T**AKALK E**T**AWALK E**T**AQALK G	Yes	No	5 – 6	N.D.
CC-Type2-$(S_aI_d)_5$	G EIAQA**S**K EIAQA**S**K EIAKA**S**K EIAWA**S**K EIAQA**S**K G	No	N.D.	N.D.	N.D.
CC-Type2-$(L_aS_d)_5$	G E**S**AQALK E**S**AQALK E**S**AKALK E**S**AWALK E**S**AQALK G	Yes	No	5 – 6	N.D.
CC-Type2-$(T_aS_d)_2$	G EIAQALK EIAQALK E**S**AKA**T**K E**S**AWA**T**K EIAQALK G	Yes	Yes	6	6YB0
Membrane-soluble	*cdefgab cdefgab cdefgab cdefgab*				
CCTM-L_bL_c	KKKKGSG I**S**AWA**T**L L**S**ALA**T**L L**S**ALA**T**L L**S**AWA**T**L G				
CCTM-V_bI_c	KKKKGSG I**S**AWA**T**V I**S**ALA**T**V I**S**ALA**T**V I**S**AWA**T**V G				
K_2-CCTM-V_bI_c	GKK **S**AWA**T**V I**S**ALA**T**V I**S**ALA**T**V I**S**AWA**T**V G				
CCTM-I_bI_c	KKKKGSG I**S**AWA**T**I I**S**ALA**T**I I**S**ALA**T**I I**S**AWA**T**I G				
CCTM-I_bL_c	KKKKGSG I**S**AWA**T**L I**S**ALA**T**L I**S**ALA**T**L I**S**AWA**T**L G				
	(Membrane-spanning region)				

a and ***d*** residues line channel/pack core.
e and ***g*** residues are interfacial (interior) and help specify the packing of hexamers.
b and ***c*** residues are interfacial (exterior) and have a minor role in defining packing.
b, ***c*** *and* ***f*** residues are exterior facing, and thus polar or apolar in water-soluble or membrane-soluble designs, respectively.

Table 1: Selected *de novo* designed peptide sequences. Polar core residues are highlighted bold. All peptides had *N*-terminal acetyl and *C*-terminal amide caps. See Supplementary Table 1 for a complete list of peptides used in this study. CC-Type2-$(L_aI_d)_4$ and CC-Type2-$(L_aI_dS_g)_4$ are described previously as CC-Hept and CC-Hex2[15].

We determined a 1.9 Å resolution X-ray crystal structure for CC-Type2-$(T_aI_d)_5$ (Fig. 1e, and Supplementary Table 2), and another for the related CC-Type2-$(T_aI_d)_2$ to 1.2 Å. These revealed parallel hexameric αHBs with internal Thr and Ile side chains in alternating layers. The hydroxyl groups of Thr stabilize small clusters of water molecules (Supplementary Fig. 5). CC-Type2-$(T_aI_d)_5$ is the first coiled coil with just one large hydrophobic residue per heptad repeat, and with an associated internal water network.

We explored the stability of this water using all-atom molecular dynamics (MD) simulations starting from a fully hydrated channel (Fig. 1h,i,j). The channel remained solvated through 1.5 μs of simulations (Fig. 1h). Moreover, water molecules exchanged freely between the channel and bulk solvent (Supplementary Fig. 6, and Supplementary Movie 1). By comparison, in similar simulations for a hexamer with all Leu at ***a*** and all Ile at ***d*** (CC-Hex2, CC-Type2-$(L_aI_dS_g)_4$,[15]) the introduced water was immediately expelled from the channel, leaving it predominantly dry (Fig. 1i, Supplementary Fig. 6, and Supplementary Movie 2).

Despite the mobility of water in the channel, we anticipated that the Ile layers of CC-Type2-$(T_aI_d)_5$ might present barriers to the passage of hydrated ions. Therefore, we tested other small polar residues at the lumenal sites (Supplementary Table 1); *e.g.*, Ser at ***a*** and ***d*** to give CC-Type2-$(S_aI_d)_5$ and CC-Type2-$(L_aS_d)_5$ (Table 1). The former was unfolded. The latter assembled into a helical oligomer (Fig. 1c,d, Table 1, and Supplementary Fig. 2,3,4). Thus, Ser residues appear better accommodated at ***d*** sites. We could not crystallize CC-Type2-$(L_aS_d)_5$. Next, we

made peptides with Thr and Ser at consecutive ***a*** at ***d*** sites. A peptide with two such heptads braced by Leu/Ile-based heptads, CC-Type2-$(T_aS_d)_2$, formed stable helical hexamers in solution (Fig. 1c,d, Table 1). This crystallized as a hexameric αHB (Fig. 1f) with a large cavity (diameter ≈7 Å, length ≈20 Å) occupied by an unusually high number (≈38) of ordered water molecules[21]. To our knowledge, this is the largest such cavity built into a *de novo* protein. The internal water molecules formed an intricate hydrogen-bonded network involving hydroxyl groups of the Ser and Thr side chains and lumen-facing backbone carbonyl groups (Fig. 1g). In MD simulations the hydrated channel was stable, and water freely exchanged in and out of it (Fig. 1j, Supplementary Fig. 6, Supplementary Movie 3).

The water-soluble barrels can be converted into membrane-spanning assemblies

To convert these water-soluble αHBs into transmembrane ion channels, we extended the Thr/Ser-based lumen of CC-Type2-$(T_aS_d)_2$ over a length required to span a membrane and increased the hydrophobicity of the exterior residues. We reasoned that multiple Thr/Ser at ***a/d*** might give stable membrane-spanning barrels because these residues promote helix-helix interactions in membranes[22]. In the resulting 'CCTM' designs, the Ala residues were retained at ***e*** and ***g***, and the exterior ***f*** positions were made Trp or Leu to match preferences for locating to headgroup and hydrocarbon regions of lipid bilayers, respectively[23] (Fig. 2a). Initially, the ***b*** and ***c*** positions were made Leu. This peptide, CCTM-L_bL_c (Table 1), had an *N*-terminal tetra-Lys tag and a *C*-terminal hydrophobic residue to promote *C*-terminal insertion into phospholipid bilayers (PLBs)[10]. Encouragingly, CCTM-L_bL_c was α helical in *n*-dodecyl β-D-maltoside (DDM) solutions (Fig. 2b and Supplementary Fig. 2k).

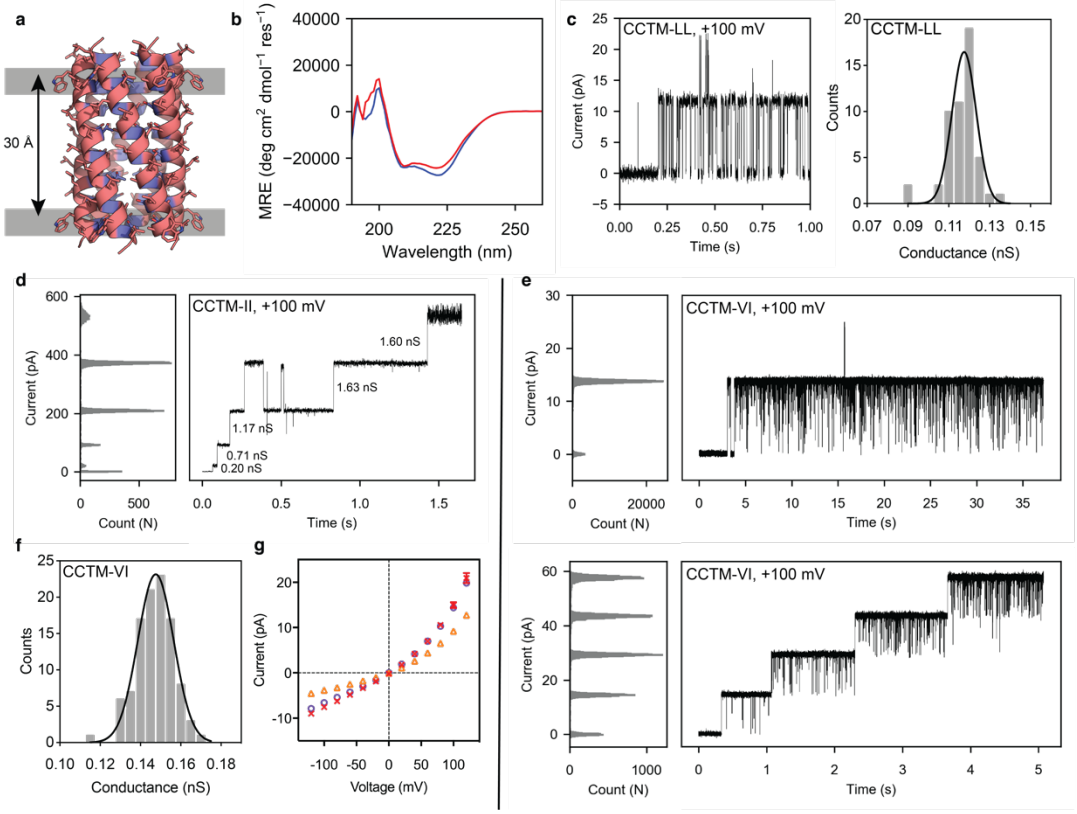

Fig. 2: Engineering and characterization of transmembrane ion-channel peptides. a, CC-Builder2 model of CCTM-L_bL_c with hydrophobic (Trp, Leu, Ala) and polar (Thr, Ser) residues coloured pink and blue, respectively. The Trp-Trp Cα distance is shown. **b**, CD spectra in 0.05% DDM at 20 ˚C for CCTM-L_bL_c (blue) and CCTM-V_bI_c (red). **c**, Insertion of CCTM-L_bL_c into a DPhPC PLB (left) and frequency distributions (right) with fitted Gaussian for this conductance (n = 51, μ = 0.12 nS, σ = 0.01 nS) at +100 mV potential in 1 M KCl. **d**, CCTM-I_bI_c channels recorded at +100 mV in 1M KCl, with the conductance values of different events labelled. **e**, Single (top) and quadruple insertions (bottom) of CCTM-V_bI_c at +100 mV. **f**, Frequency distribution histogram for CCTM-V_bI_c channels (n = 104, μ = 0.15 nS, σ = 0.01 nS) at +100 mV in 1 M KCl. **g**, Current-voltage curves for single CCTM-V_bI_c channels. Electrolyte: 1 M each of KCl (purple), NaCl (orange) or CsCl (red). Buffer: 10 mM Tris-HCl, pH 8.0.

For all experiments, peptide concentrations in the *cis* compartment were 50 nM, and signals were acquired at 10 kHz and low-pass filtered at 2 kHz.

To test for functional ion channels, we used single-channel electrical recordings across diphytanoyl-*sn*-glycero-3-phosphocholine (DPhPC) PLBs at +100 mV in 1 M KCl. CCTM-L_bL_c was added from micellar solutions to the *cis* (ground) side of the bilayer. This diluted the solutions below their critical micelle concentration. The formation of individual channels was evident from uniform steps in ionic current of ≈12 pA (Fig. 2c, and Supplementary Fig. 7), corresponding to ≈7.5 x 10^7 ions/sec. Based on this, conductance histograms (Fig. 2c) confirmed homogeneous channels with a unitary conductance of ≈0.12 nS.

Using a computational coiled-coil design method[15] (Supplementary Methods), we explored the effect on ion-channel properties of placing different hydrophobic residues at ***b*** and ***c*** to optimize helix-helix packing[4]. The top-scoring sequences had Val/Ile, Ile/Ile and Leu/Ile combinations at ***b/c*** (Supplementary Table 3). In single-channel PLB experiments, the peptides with Ile/Ile and Leu/Ile at ***b/c*** formed channels that no longer had a single conductance but showed increasingly large steps in current (Fig. 2d). This is reminiscent of alamethicin pores, which increase oligomeric state by sequential additions of peptide[24]. By contrast, channels formed by CCTM-V_bI_c (with Val/Ile at ***b/c***; Fig. 2e,f) were monodisperse, longer-lived than for CCTM-L_bL_c or foregoing *de novo* peptide channels[9], and exhibited less gating (Fig. 2, and Supplementary Fig. 7).

All of the CCTM peptides were α helical in DDM solutions (Supplementary Figs. 2l-o). In AUC experiments, the two variants of CCTM-V_bI_c (Table 1) clearly associated in detergent solutions (Supplementary Figs. 3f and 3g). However, the sizes of the oligomers formed depended on the variant and the detergent used. In our understanding, AUC of pore-forming peptides with association states larger than four or five is notoriously difficult, and there are no reports of such experiments that reveal the assembly of an active barrel-stave-pore state.

CCTM-V_bI_c forms antiparallel helical bundles in the lipidic cubic phase

Despite the difficulties encountered with AUC, having derived a CCTM design with favourable ion-channel properties we sought to solve its structure. A 2.1 Å resolution X-ray structure was determined for K_2-CCTM-V_bI_c (Table 1) crystallized from the lipidic cubic phase (LCP)[25]. This confirmed a bundle of amphipathic α helices with Type-2 KIH packing involving most ***a***, ***d***, ***e*** and ***g*** sites (Fig. 3a,b, and Supplementary Table 4). Surprisingly, however, the structure had two antiparallel 4-helix bundles associated laterally to form an octamer (Fig. 3a,b). While at odds with our target of a parallel αHB, we sought to reconcile this observation with sequence features of the CCTM-V_bI_c.

The CCTM-V_bI_c sequence has small Ala and Ser residues each spaced seven residues apart. These are the hallmarks of alanine and serine zippers, which have tightly packed antiparallel helices[26-28]. The observed structure appears to maximise the number of these zippers (Fig. 3c), and it allows the Ser and Thr residues to form an extensive hydrogen-bonded network. However, this leaves space for only a few isolated pairs of water molecules (Fig. 3d). The lack of a more substantial pore hints that this conformation is not the active ion-conducting state of CCTM-V_bI_c (see below), but an alternative state accessible on the free-energy landscape for the peptide sequence. Similar antiparallel structures are known. For example, the water-soluble peptide CC-Hex-L24E crystallises as either a parallel 6-helix αHB or an antiparallel tetramer, depending on conditions[29]. Hence, both structures are accessible to CCTM-V_bI_c, and likely close in energy. In addition, the few available X-ray structures of natural membrane-spanning pore-forming α-helical peptides have antiparallel helices[30-32], though these are not necessarily the active states[33].

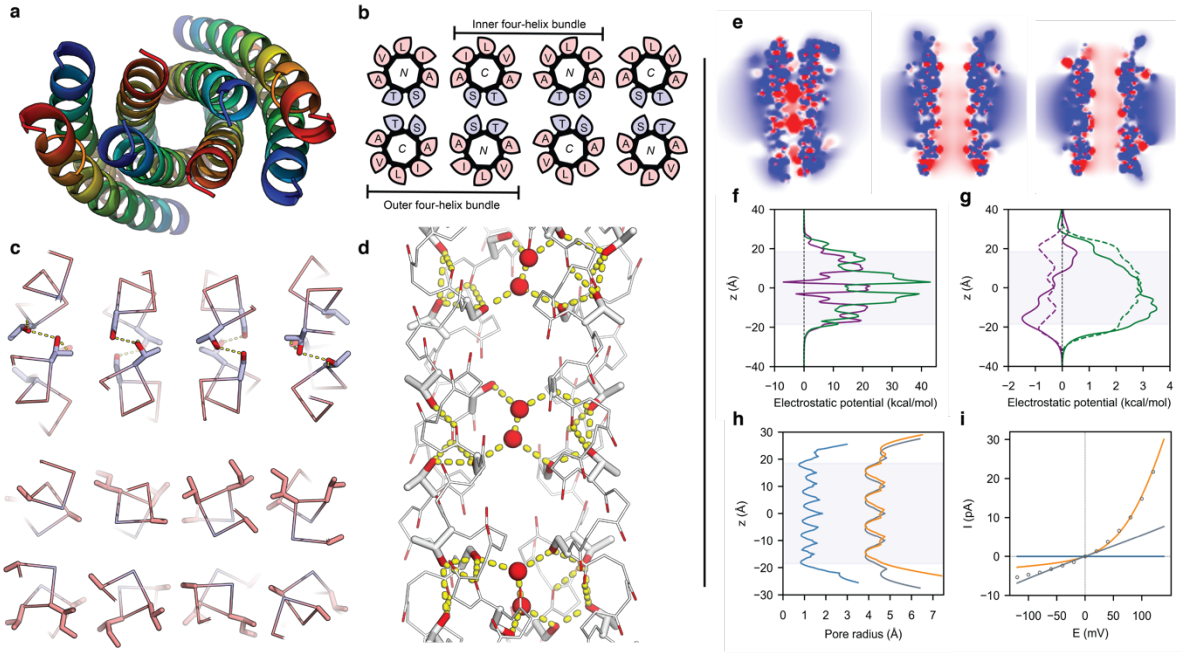

Fig. 3: LCP crystal structure of K_2-CCTM-V_bI_c and modelling of alternate states. *N.B.* This structure is of a variant with a Lys_2 rather than a Lys_4 *N*-terminal tag; both peptides had similar biophysical and conductance properties (Supplementary Fig. 7b). **a**, Axial view of the octameric assembly. **b**, Corresponding helical wheels showing two distinct four-helix bundles. The inner bundle has a hydrophobic interior of methyl groups from Ala and Thr; whereas, the outer bundles are hydrophilic, lined with hydroxyl groups of Ser and Thr. **c**, A hydrogen-bonded layer of Thr/Ser at ***a/d*** (top) and the same layer showing the hydrophobic interfaces with Ala at ***e*** and ***g***, and Val/Ile at ***b/c*** (bottom). **d**, Hydrogen-bonding network within the outer bundle involving isolated water molecules, Thr/Ser side chains, and backbone carbonyls. Hydrogen bonds (yellow dashes) are for O-O distances <3 Å. **e**, Slices through the isosurfaces, in the absence of an applied potential, of the outer four-helix bundle of the experimental octamer (left) and for models of a parallel hexamer (centre) and an antiparallel hexamer (right) of K_2-CCTM-V_bI_c. These are coloured from red to blue for $-8\ k_bT/e_c$ to $8\ k_bT/e_c$, and indicate internal negative electrostatic potentials consistent with cation selectivity. **f,g,** Calculated electrostatic potential energies for moving K^+ (purple) and Cl^- (green) through the channels of the outer four-helix bundle (**f**) and the hexameric models (**g**; parallel, solid lines; antiparallel, dotted lines). **h**, Calculated channel radii for the outer four-helix bundle of the octamer (blue), the hexameric models (parallel, orange; antiparallel, grey). **i**, Calculated I-V curves for the four-helix bundle (blue), the hexamers (parallel, orange; antiparallel, grey), with the experimental data shown as points.

CCTM-V_bI_c forms well-defined ion-channels in planar-lipid membranes

The apparent contradiction between the crystal structure of K_2-CCTM-V_bI_c and its channel properties in lipid bilayers led us to make further electrical recordings.

Single CCTM-V_bI_c channels had a unitary conductance of 0.15 ± 0.01 nS (+100 mV, 1 M KCl, Fig. 2f), corresponding to ≈9 x 10^7 ions/sec, a high conductance for synthetic peptide channels[9]. This suggests a channel diameter of ≈10 Å[34], far closer to that predicted for the water-soluble hexamer, CC-Type2-$(T_aS_d)_2$, than to the four-helix bundles of the octamer (see below). Reversal potential measurements showed that the channels were cation-selective, with a permeability ratio of ≈5:1 for K^+ versus Cl^- (Supplementary Fig. 7), consistent with the solvation of cations by hydroxyl groups of Ser/Thr-lined channels. CCTM-V_bI_c also conducted Na^+ and Cs^+, and current-voltage curves obtained in different electrolytes were non-linear with marked current rectification (Fig. 2g). Such rectification arises from asymmetric charge distributions[35,36]. This is consistent with a parallel assembly of helices with *N*-terminal Lys tags, but not with the antiparallel arrangement seen in the LCP structure of K_2- CCTM-V_bI_c (see below).

In addition, we performed simultaneous electrical and optical single-channel recording, oSCR[24,37,38], monitoring the flux of calcium ions through individual CCTM-V_bI_c channels inserted into DPhPC droplet-interface bilayers (DIBs; Fig. 4 and Supplementary Fig. 8)[39].

Electrically, as in PLBs, CCTM-V_bI_c showed discrete unitary conductance in DIBs (Fig. 4b). Optically, the calcium flux imaging showed multiple mobile spots diffusing in the plane of the bilayer, indicative of transmembrane channels (Fig. 4c & Supplementary Movie 4). The fluorescence from these isolated channels showed single distinct open and closed states, further demonstrating the unitary conductance of the CCTM-V_bI_c channels (Fig. 4d,e).

Direct imaging of a Cyanine 5-labelled peptide, Cy5-CCTM-V_bI_c, showed it diffused across the entire membrane, including regions away from the channels seen by oSCR (Supplementary Fig. 8). These species had a mean lateral diffusion coefficient (D_{lat}) of 2.56 ± 0.99 $\mu m^2 s^{-1}$, similar to monomeric transmembrane helices in related membranes[40]. However, the Ca^{2+}-conducting channels diffused more slowly (D_{lat} = 1.05 ± 0.26 $\mu m^2 s^{-1}$, similar to multi-peptide alamethicin pores[24]). Using these D_{lat} values in the Saffman-Delbrück equation[41], we estimated an approximate 4-fold increase in diameter between the individual peptides and the conductive channels (Supplementary Fig. 8). Although this carries assumptions, it is consistent with the relative sizes of helical monomers and αHBs[15].

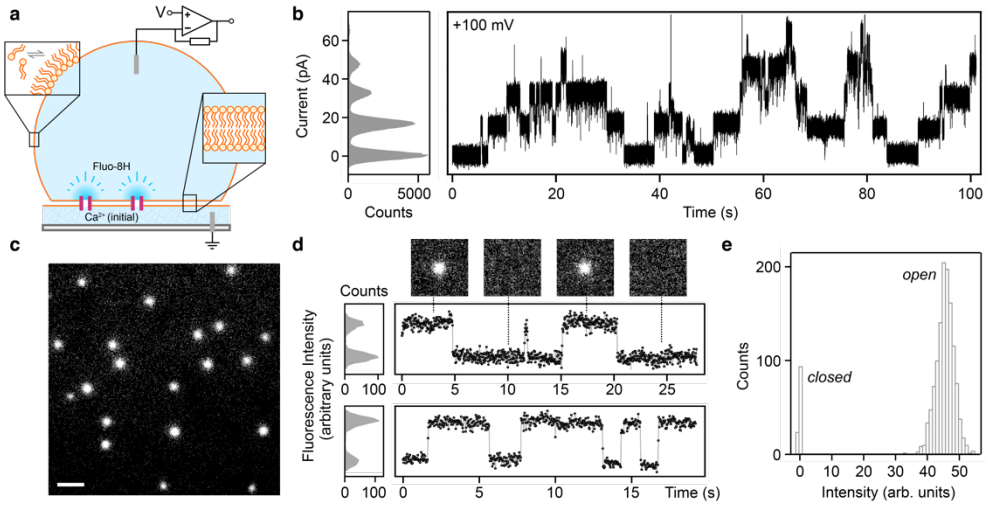

Fig. 4: CCTM-V_bI_c channels in droplet-interface bilayers. a, Cartoon of a DIB formed between an aqueous droplet and a hydrogel substrate spun onto a coverslip (grey), both in the presence of a lipid-in-oil solution. The DIB has Ca^{2+} ions in the hydrogel and the Ca^{2+}-sensitive dye Fluo-8H in the droplet. Channels (purple blocks) formed in the bilayer allow passage of Ca^{2+} ions into the droplet to generate plumes of Ca^{2+}-bound dye (depicted in darker blue) that can be imaged using TIRF microscopy. **b**, Conductance steps from multiple insertions of CCTM-V_bI_c in a DIB at +100 mV. Voltages are *trans* relative to *cis* (peptide). **c,** oSCR for CCTM-V_bI_c channels in a DPhPC membrane at +100 mV. This is a single 30 ms exposure; 100 nM CCTM-V_bI_c; scale bar, 10 μm. **d**, Fluorescence intensity versus time traces for two CCTM-V_bI_c channels. The y-axes represent mean pixel values of bilayer patches containing the channels. The upper trace is annotated with 30 ms frames (17.8 μm x 17.8 μm) from the respective oSCR image stack. **e**, Spot intensities extracted from eight CCTM-V_bI_c channels in the same bilayer, which represent 40 s of open-channel time, show a unitary open state and a closed state. For all experiments, the droplet peptide concentrations were between 25 nM and 100 nM.

Computational analyses of possible antiparallel and parallel states of CCTM-V_bI_c

Finally, to help distinguish between the possible states that CCTM-V_bI_c might form in the membrane, we performed simulations and *in silico* calculations on the K_2-CCTM-V_bI_c structure, *i.e.* the dimer of antiparallel 4-helix bundles, and with the peptide modelled as parallel and antiparallel hexamers (Fig. 3e-i). Hexamers were chosen to match the oligomeric state of the water-soluble parent and consistent with the conductance data. The models were generated in CCBuilder2[19] using parameters from CC-Type2-$(T_aS_d)_2$ X-ray crystal structure.

In contrast to simulations for the water-soluble barrels (Fig. 1h,i,j), MD studies of the K_2-CCTM-V_bI_c octamer in DPhPC bilayers indicated that very few water molecules traversed the channel or exchange with bulk solvent (Supplementary Fig. 9, and Supplementary Movie 5). Rather, and consistent with the ordered crystallographic water, water molecules remained bound to internal Ser and Thr side chains of the outer four-helix bundles for hundreds of nanoseconds

(Supplementary Table 5). In short, these interiors were rarely solvated across their full lengths. Moreover, ions included in different simulations (*e.g.*, Ca^{2+}, Na^{+}, K^{+}, Cl^{-}) did not enter these spaces over a cumulative 3.2 µs of simulation. *N.B.* The interior of the inner four-helix bundle remained dry in all simulations.

Poisson-Boltzmann electrostatic calculations using APBSmem[42] supported these findings (Fig. 3e, and Supplementary Fig. 10): The calculated electrostatic potential energy barriers for the outer four-helix bundle of the octameric crystal structure were too high to conduct K^{+} or Cl^{-} (Fig. 3f). However, the barriers calculated for the parallel hexameric model were an order of magnitude lower and similar to those calculated for natural ion channels (Fig. 3g)[43]. We attribute this to the different diameters of the cavities in the four- and six-helix models (Fig. 3h). The K^{+}/Cl^{-} selectivity observed experimentally was manifest in the calculations as a lower energy profile for K^{+} compared with Cl^{-} for the hexamers (Fig. 3g), which we attribute to the hydroxyl groups lining the channel. Finally, we modelled the current-voltage relationship using Nernst-Plank electrodiffusion theory[34]. The computed I-V curve for the parallel hexameric model agreed qualitatively with the current rectification observed experimentally (Fig. 2g, 3i, and Supplementary Fig. 10). By contrast, the calculated I-V plot for the antiparallel hexameric model was linear; and no current was predicted for the octameric crystal structure across the voltage range. From these analyses, we propose an all-parallel barrel-like structure, possibly a hexamer, as the most-likely open-channel state.

Conclusion

We have shown that multiple polar residues can be incorporated within the lumens of water-soluble, *de novo* α-helical barrels (αHBs). The combination of ***a*** = Ser and ***d*** = Thr in ***a→g*** sequence repeats generates large cavities that sequester water molecules that freely exchange with bulk water. This background can be used to generate ion-conducting membrane-spanning peptides by introducing hydrophobic residues at the ***b***, ***c*** and ***f*** sites. One of these CCTM peptides forms discrete and stable ion channels in membranes. Designed peptide channels with this degree of stability and monodispersity are unprecedented and reminiscent of those formed by the engineered natural peptides cWza and pPorA[10,44]. This demonstrates how consideration of helix-helix packing and lumen design can deliver membrane-spanning assemblies with defined ion-channel activities.

That said, the peptides that we have made accesses multiple states. One of our CCTM peptides crystallizes from the lipidic cubic phase (LCP) as a dimer of an antiparallel tetramer, while in membranes under voltage both monomeric peptides and assembled channels are observed. The antiparallel tetramers are unlikely to be the channel state: although they have polar interiors, these are too narrow to conduct ions or even water; and their dihedral symmetry is inconsistent with rectification observed for the conducting state. Given this, we propose the following model for CCTM activity, though we recognise that different membrane mimics may result in different assemblies. In the lipidic cubic phase, the antiparallel structure is a low-energy, readily accessible state. By contrast, in planar lipid bilayers the peptide forms an equilibrium of monomeric and oligomeric species. The voltage applied to record channel currents may aid in establishing the channels, either by increasing local peptide concentration or thinning the membrane. However, in DIBs, peptide concentrations of 100 – 350 nM give currents from hundreds of channels even at low voltage (10 – 20 mV), suggesting that channels insert readily. For the conducting state, we propose a parallel α-helical barrel-stave structure with a solvent-accessible central channel similar to those seen in the water-soluble parent peptides. This multi-state behaviour mimics natural channel-forming peptides, the structures of which are often condition-dependent[33].

Of course, without a high-resolution structure of the conducting state, we cannot be certain of this model. Given the apparent structural plasticity of the system, it may prove difficult to obtain such a structure. It may be possible to stabilise the active state through templating[45], or to

employ negative design to destabilise the alternate state(s)[46]. However, the generation of stable barrel-stave structures of peptide helices may continue to prove challenging. Indeed, we find that water-soluble αHBs collapse without key sequence features[18]. We observe something similar in the LCP structure of CCTM, where close packing of the Ala, Ser, Thr core residues leads to the dimer of four-helix bundles. Furthermore, it is interesting that although nature has evolved stable membrane-spanning αHBs that are crystallisable, these are usually templated by extra-membranous domains or buttressed by concentric rings of helices in the membrane[47,48]. Further still, many natural membrane pores are assembled from multiple β-hairpin units[47,49]. Although extremely large barrels appear to be accessible through this mode of assembly, again they are often templated by large water-soluble domains. Efforts to design even water-soluble β-barrel systems are in their infancy[50], and carry the added challenge of avoiding amyloid states.

Thus, whilst our work and examples of natural membrane-spanning αHBs offer hope for designing such assemblies, they do not completely solve the problem of how to specify peptide-peptide interactions to generate barrel-stave structures that are stable over broad conditions. Nonetheless, we have achieved considerable control over self-assembly in water and function in membranes. Improving on this further would increase understanding of natural channel and pore-forming peptides, provide further principles for designing peptide ion channels, and, ultimately, unlock applications for these in biotechnology[49].

References

1 Huang, P. S., Boyken, S. E. & Baker, D. The coming of age of de novo protein design. *Nature* **537**, 320-327 (2016).
2 Korendovych, I. V. & DeGrado, W. F. De novo protein design, a retrospective. *Q. Rev. Biophys.* **53**, e3 (2020).
3 Lu, P. L. *et al.* Accurate computational design of multipass transmembrane proteins. *Science* **359**, 1042-1046 (2018).
4 Mravic, M. *et al.* Packing of apolar side chains enables accurate design of highly stable membrane proteins. *Science* **363**, 1418-1423 (2019).
5 Joh, N. H. *et al.* De novo design of a transmembrane Zn2+-transporting four-helix bundle. *Science* **346**, 1520-1524 (2014).
6 Davey, J. A., Damry, A. M., Goto, N. K. & Chica, R. A. Rational design of proteins that exchange on functional timescales. *Nat. Chem. Biol.* **13**, 1280-1285 (2017).
7 Chen, K. Y. M., Keri, D. & Barth, P. Computational design of G Protein-Coupled Receptor allosteric signal transductions. *Nat. Chem. Biol.* **16**, 77-86 (2020).
8 Woolfson, D. N. Coiled-Coil Design: Updated and Upgraded. *Subcell. Biochem.* **82**, 35-61 (2017).
9 Lear, J. D., Wasserman, Z. R. & Degrado, W. F. Synthetic Amphiphilic Peptide Models for Protein Ion Channels. *Science* **240**, 1177-1181 (1988).
10 Mahendran, K. R. *et al.* A monodisperse transmembrane alpha-helical peptide barrel. *Nat Chem* **9**, 411-419 (2017).
11 Bowie, J. U. Helix packing in membrane proteins. *J. Mol. Biol.* **272**, 780-789 (1997).
12 Hong, H. Toward understanding driving forces in membrane protein folding. *Arch. Biochem. Biophys.* **564**, 297-313 (2014).
13 Liu, J. *et al.* A seven-helix coiled coil. *Proc. Natl. Acad. Sci. U.S.A.* **103**, 15457-15462 (2006).
14 Zaccai, N. R. *et al.* A de novo peptide hexamer with a mutable channel. *Nat. Chem. Biol.* **7**, 935-941 (2011).
15 Thomson, A. R. *et al.* Computational design of water-soluble alpha-helical barrels. *Science* **346**, 485-488 (2014).
16 Krivov, G. G., Shapovalov, M. V. & Dunbrack, R. L. Improved prediction of protein side-chain conformations with SCWRL4. *Proteins* **77**, 778-795 (2009).

17 Klesse, G., Rao, S. L., Sansom, M. S. P. & Tucker, S. J. CHAP: A Versatile Tool for the Structural and Functional Annotation of Ion Channel Pores. *J. Mol. Biol.* **431**, 3353-3365 (2019).

18 Rhys, G. G. *et al.* Maintaining and breaking symmetry in homomeric coiled-coil assemblies. *Nat. Commun.* **9**, ARTN 4132 (2018).

19 Wood, C. W. & Woolfson, D. N. CCBuilder 2.0: Powerful and accessible coiled-coil modeling. *Protein Sci.* **27**, 103-111 (2018).

20 Walshaw, J. & Woolfson, D. N. SOCKET: A program for identifying and analysing coiled-coil motifs within protein structures. *J. Mol. Biol.* **307**, 1427-1450 (2001).

21 Carugo, O. Statistical survey of the buried waters in the Protein Data Bank. *Amino Acids* **48**, 193-202 (2016).

22 Dawson, J. P., Weinger, J. S. & Engelman, D. M. Motifs of serine and threonine can drive association of transmembrane helices. *J. Mol. Biol.* **316**, 799-805 (2002).

23 Hessa, T. *et al.* Molecular code for transmembrane-helix recognition by the Sec61 translocon. *Nature* **450**, 1026-1030 (2007).

24 Harriss, L. M., Cronin, B., Thompson, J. R. & Wallace, M. I. Imaging Multiple Conductance States in an Alamethicin Pore. *J. Am. Chem. Soc.* **133**, 14507-14509 (2011).

25 Landau, E. M. & Rosenbusch, J. P. Lipidic cubic phases: A novel concept for the crystallization of membrane proteins. *Proc. Natl. Acad. Sci. U.S.A.* **93**, 14532-14535 (1996).

26 Gernert, K. M., Surles, M. C., Labean, T. H., Richardson, J. S. & Richardson, D. C. The Alacoil - a Very Tight, Antiparallel Coiled-Coil of Helices. *Protein Sci.* **4**, 2252-2260 (1995).

27 Adamian, L. & Liang, J. Interhelical hydrogen bonds and spatial motifs in membrane proteins: Polar clamps and serine zippers. *Proteins* **47**, 209-218 (2002).

28 Zhang, S. Q. *et al.* The Membrane- and Soluble-Protein Helix-Helix Interactome: Similar Geometry via Different Interactions. *Structure* **23**, 527-541 (2015).

29 Rhys, G. G. *et al.* Navigating the Structural Landscape of De Novo alpha-Helical Bundles. *J. Am. Chem. Soc.* **141**, 8787-8797 (2019).

30 Song, C. *et al.* Crystal structure and functional mechanism of a human antimicrobial membrane channel. *Proc. Natl. Acad. Sci. U.S.A.* **110**, 4586-4591 (2013).

31 Hayouka, Z. *et al.* Quasiracemate Crystal Structures of Magainin 2 Derivatives Support the Functional Significance of the Phenylalanine Zipper Motif. *J. Am. Chem. Soc.* **137**, 11884-11887 (2015).

32 Kurgan, K. W. *et al.* Retention of Native Quaternary Structure in Racemic Melittin Crystals. *J. Am. Chem. Soc.* **141**, 7704-7708 (2019).

33 Sansom, M. S. P. The Biophysics of Peptide Models of Ion Channels. *Prog. Biophys. Mol. Bio.* **55**, 139-235 (1991).

34 Hille, B. *Ionic Channels of Excitable Membranes*. (Oxford University Press, 2001).

35 Kienker, P. K., Degrado, W. F. & Lear, J. D. A Helical-Dipole Model Describes the Single-Channel Current Rectification of an Uncharged Peptide Ion-Channel. *Proc. Natl. Acad. Sci. U.S.A.* **91**, 4859-4863 (1994).

36 Noskov, S. Y., Im, W. & Roux, B. Ion permeation through the alpha-hemolysin channel: Theoretical studies based on Brownian dynamics and Poisson-Nernst-Plank electrodiffusion theory. *Biophys. J.* **87**, 2299-2309 (2004).

37 Wang, S. Q., Song, L. S., Lakatta, E. G. & Cheng, H. P. Ca2+ signalling between single L-type Ca2+ channels and ryanodine receptors in heart cells. *Nature* **410**, 592-596 (2001).

38 Heron, A. J., Thompson, J. R., Cronin, B., Bayley, H. & Wallace, M. I. Simultaneous Measurement of Ionic Current and Fluorescence from Single Protein Pores. *J Am Chem Soc* **131**, 1652-1653 (2009).

39 Leptihn, S. *et al.* Constructing droplet interface bilayers from the contact of aqueous droplets in oil. *Nat. Protoc.* **8**, 1048-1057 (2013).

40 Ramadurai, S., Duurkens, R., Krasnikov, V. V. & Poolman, B. Lateral Diffusion of Membrane Proteins: Consequences of Hydrophobic Mismatch and Lipid Composition. *Biophys. J.* **99**, 1482-1489 (2010).
41 Saffman, P. G. & Delbruck, M. Brownian-Motion in Biological-Membranes. *Proc. Natl. Acad. Sci. U.S.A.* **72**, 3111-3113 (1975).
42 Callenberg, K. M. *et al.* APBSmem: A Graphical Interface for Electrostatic Calculations at the Membrane. *Plos One* **5**, ARTN e12722 (2010).
43 Roux, B., Allen, T., Berneche, S. & Im, W. Theoretical and computational models of biological ion channels. *Q. Rev. Biophys.* **37**, 15-103 (2004).
44 Krishnan, R. S. *et al.* Autonomously Assembled Synthetic Transmembrane Peptide Pore. *J. Am. Chem. Soc.* **141**, 2949-2959 (2019).
45 Spruijt, E., Tusk, S. E. & Bayley, H. DNA scaffolds support stable and uniform peptide nanopores. *Nat. Nanotechnol.* **13**, 739-745 (2018).
46 Grigoryan, G., Reinke, A. W. & Keating, A. E. Design of protein-interaction specificity gives selective bZIP-binding peptides. *Nature* **458**, 859-864 (2009).
47 Dal Peraro, M. & van der Goot, F. G. Pore-forming toxins: ancient, but never really out of fashion. *Nat. Rev. Microbiol.* **14**, 77-92 (2016).
48 Niitsu, A., Heal, J. W., Fauland, K., Thomson, A. R. & Woolfson, D. N. Membrane-spanning alpha-helical barrels as tractable protein-design targets. *Philos. T. R. Soc. B* **372**, ARTN 20160213 (2017).
49 Howorka, S. Building membrane nanopores. *Nat. Nanotechnol.* **12**, 619-630 (2017).
50 Dou, J. Y. *et al.* De novo design of a fluorescence-activating beta-barrel. *Nature* **561**, 485-491 (2018).

Acknowledgements
A.J.S. thanks Diamond Light Source for a place on the CCP4 Data Collection and Structure Solution Workshop 2017. E.J.M.L. thanks Shanlin Rao and Gianni Klesse (University of Oxford) for support with CHAP and Frank Marcoline (UCSF) for support with APBSmem. A.J.S. was funded by the Bristol Chemical Synthesis Centre for Doctoral Training funded by the EPSRC (EP/G036764/1). A.N. and K.R.M. were supported by a BBSRC grant to R.L.B., H.B. and D.N.W (BB/J009784/1). W.M.D., A.N., A.J.S., A.R.T. and D.N.W. were funded by ERC Grants to D.N.W. (340764 and 787173). E.J.M.L. was in the BBSRC/EPSRC-funded Synthetic Biology Research Centre, BrisSynBio ((BB/L01386X/1). M.I.W. was funded by the BBSRC (BB/R001790/1). W.F.D. was supported by NIH (R35 GM122603), NSF (1709506), US Air Force (1709506) grants. H.T.K. was supported by the NIH Ruth L. Kirschstein NRSA Postdoctoral Fellowship (F32GM125217). M.M. is supported by the Howard Hughes Medical Institute Gilliam Fellowship. D.N.W. held a Royal Society Wolfson Research Merit Award (WM140008).

Author contributions
A.J.S., A.N., K.R.M., A.R.T. H.B., R.L.B. and D.N.W. conceived the project and designed the peptides, which A.J.S., A.N. and W.M.D. synthesized. A.J.S., A.N. and K.R.M performed solution-phase biophysics and electrophysiology experiments. A.J.S., H.T.K. and L.L. determined X-ray crystal structures. A.J.S. and A.R.T. did the computational design. E.J.M.L., M.M. and A.J.M. ran and analysed the MD simulations. E.J.M.L. conducted the electrostatic calculations. J.T.S. and M.I.W. conducted and analysed the oSCR. A.J.S., E.J.M.L. and D.N.W. wrote the manuscript, to which all authors contributed.

Competing interests
None.

Supplementary materials
Supplementary Information Figs. 1 to 10**;** Supplementary Tables 1 to 5**;** Supplementary Movies 1 to 5.

Crystallographic data

X-ray crystal structures have been submitted to the RCSB Protein Data Bank with accession codes 6YAZ, 6YB0, 6YB1, and 6YB2.